(This is a sample cover image for this issue. The actual cover is not yet available at this time.)

Earth and Planetary Science Letters 355-356 (2012) 174–186

Contents lists available at SciVerse ScienceDirect

Earth and Planetary Science Letters

journal homepage: www.elsevier.com/locate/epsl

Solar and climate influences on ice core ^{10}Be records from Antarctica and Greenland during the neutron monitor era

J.B. Pedro [a,b,*], J.R. McConnell [c], T.D. van Ommen [b,d], D. Fink [e], M.A.J. Curran [b,d], A.M. Smith [e], K.J. Simon [e], A.D. Moy [b,d], S.B. Das [f]

[a] Institute of Marine and Antarctic Studies, University of Tasmania, Hobart, TAS, Australia
[b] Antarctic Climate & Ecosystems Cooperative Research Centre, University of Tasmania, Hobart, TAS, Australia
[c] Desert Research Institute, Reno, NV, USA
[d] Australian Antarctic Division, Kingston, TAS, Australia
[e] Australian Nuclear Science and Technology Organisation, Menai, NSW, Australia
[f] Woods Hole Oceanographic Institution, Woods Hole, MA, USA

ARTICLE INFO

Article history:
Received 28 January 2012
Received in revised form
17 July 2012
Accepted 22 August 2012
Editor: G. Henderson

Keywords:
cosmogenic ^{10}Be
beryllium-10
ice core
solar activity
climate
North Atlantic Oscillation

ABSTRACT

Cosmogenic ^{10}Be in polar ice cores is a primary proxy for past solar activity. However, interpretation of the ^{10}Be record is hindered by limited understanding of the physical processes governing its atmospheric transport and deposition to the ice sheets. This issue is addressed by evaluating two accurately dated, annually resolved ice core ^{10}Be records against modern solar activity observations and instrumental and reanalysis climate data. The cores are sampled from the DSS site on Law Dome, East Antarctica (spanning 1936–2009) and the Das2 site, southeast Greenland (1936–2002), permitting inter-hemispheric comparisons. Concentrations at both DSS and Das2 are significantly correlated to the 11-yr solar cycle modulation of cosmic ray intensity, $r_{xy} = 0.54$ with 95% CI [0.31; 0.70], and $r_{xy} = 0.45$ with 95% CI [0.22; 0.62], respectively. For both sites, if fluxes are used instead of concentrations then correlations with solar activity decrease. The strength and spectral coherence of the solar activity signal in ^{10}Be is enhanced when ice core records are combined from both Antarctica and Greenland. The amplitudes of the 11-yr solar cycles in the ^{10}Be data appear inconsistent with the view that the ice sheets receive only ^{10}Be produced at polar latitudes. Significant climate signals detected in the ^{10}Be series include the zonal wave three pattern of atmospheric circulation at DSS, $r_{xy} = -0.36$ with 95% CI [−0.57; −0.10], and the North Atlantic Oscillation at Das2, $r_{xy} = -0.42$ with 95% CI [−0.64; −0.15]. The sensitivity of ^{10}Be concentrations to modes of atmospheric circulation advises caution in the use of ^{10}Be records from single sites in solar forcing reconstructions.

1. Introduction

The atmospheric production rate of cosmogenic ^{10}Be is proportional to cosmic ray intensity, which in turn is modulated by variations in solar activity and the Earth's geomagnetic field strength (Lal and Peters, 1967). This relationship is exploited in the use of ^{10}Be records from polar ice cores to reconstruct solar activity prior to the era of instrumental records (e.g. Bard et al., 2000; Vonmoos et al., 2006; Muscheler et al., 2007b; Usoskin et al., 2009; Delaygue and Bard, 2011; Shapiro et al., 2011; Steinhilber et al., 2012). Such reconstructions provide crucial information for assessing the role of solar forcing in past climate change (e.g. Bard et al., 2000; Steinhilber et al., 2012) and for attributing present climate change (e.g. Ammann et al., 2007). However, different solar reconstructions are not all in agreement and the reliability of ^{10}Be as a solar proxy has sometimes been questioned (Lal, 1987; Webber and Higbie, 2010).

^{10}Be is produced by interactions between N and O atoms and secondary particles of the cosmic-ray induced atmospheric cascade (Lal and Peters, 1967). Globally, ~60−70% of the columnar production occurs in the stratosphere, with the remainder in the upper troposphere (e.g. Masarik and Beer, 2009; Kovaltsov and Usoskin, 2010). Following production, it is assumed (due to its valence charge, small ionic radius and strong chemical adsorption affinity) that ^{10}Be is rapidly scavenged by ambient aerosol then transported with air-masses (Igarashi et al., 1998; Aldahan et al., 2008). Observational and modeling studies report atmospheric residence times for the aerosol-bound ^{10}Be of ~1 yr in the stratosphere and several weeks in the troposphere before deposition to the Earth's surface (e.g. Raisbeck et al., 1981; Jordan et al., 2003; Heikkilä et al., 2009; Pedro et al., 2011a).

Key factors limiting the reliability of ^{10}Be-based solar reconstructions include (1) the confounding effect of non-production related signals introduced during the atmospheric transport and deposition

* Corresponding author at: Institute of Marine and Antarctic Studies, University of Tasmania, Hobart, TAS, Australia.
E-mail address: jbpedro@utas.edu.au (J.B. Pedro).

0012-821X/$ - see front matter © 2012 Elsevier B.V. All rights reserved.
http://dx.doi.org/10.1016/j.epsl.2012.08.038

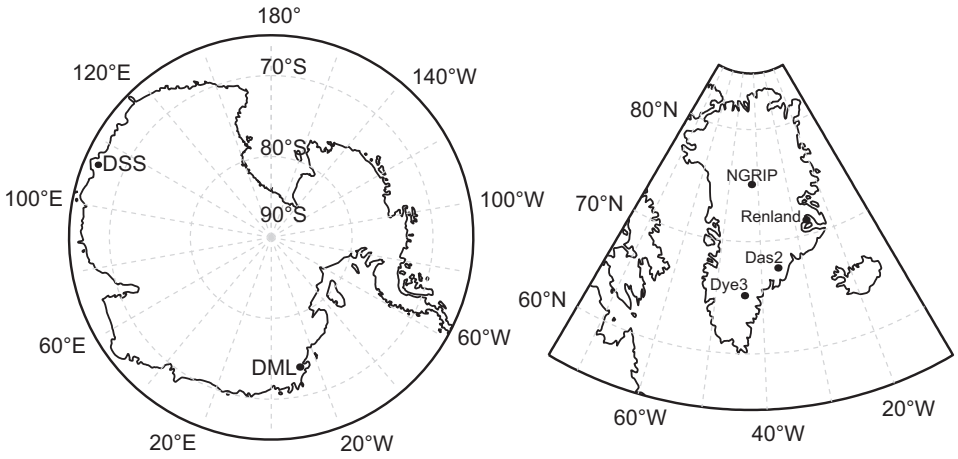

Fig. 1. Map showing the location of the DSS (Law Dome Summit South) and Das2, southeast Greenland ice core sites from which the new ^{10}Be records presented in the text were obtained. The locations of additional ice core ^{10}Be records used in the bipolar ^{10}Be composite are also shown: DML (Dronning Maud Land), Renland, NGRIP and Dye 3.

of the isotope to the ice sheets (e.g. Lal, 1987; Pedro et al., 2006; Field et al., 2006; Field and Schmidt, 2009; Pedro et al., 2011b; Baroni et al., 2011) and (2) debate about where in the atmosphere the ^{10}Be deposited to the ice core sites is produced (e.g. Mazaud et al., 1994; Steig et al., 1996; Bard et al., 1997; Field et al., 2006; Heikkilä et al., 2009; Muscheler and Heikkilä, 2011). The first factor is critical since incorrectly attributing climate-induced signals in ^{10}Be to changes in solar activity risks drawing false conclusions about solar forcing of climate. The second factor is important since different assumptions regarding atmospheric source regions directly affect the amplitudes of reconstructed solar variations. Here we address this issue through direct intercomparison of annually resolved and accurately dated ice core ^{10}Be data with modern instrumental records.

Two new ^{10}Be records are presented, one from the DSS site, Law Dome, East Antarctica and one from the Das2 site, southeast Greenland (see Fig. 1 for locations). The exceptionally high snow accumulation rates at both sites, 0.68 m ice yr^{-1} at DSS (Morgan et al., 1997) and 0.90 m ice yr^{-1} at Das2 (Hanna et al., 2006), preserve thick and clear annual snow layers permitting unambiguous dating of the records. To assess the strength of production signals the measured concentrations and calculated ^{10}Be fluxes are evaluated against cosmic ray intensities as recorded by ground-based neutron monitors since the 1950s and also against modeled atmospheric ^{10}Be production rates (Kovaltsov and Usoskin, 2010). Potential climate signals are examined through intercomparison of the ^{10}Be data with climate variables for which there is an a priori reason to suspect an influence on ^{10}Be deposition or transport: (i) observed accumulation rates; (ii) dominant modes of atmospheric circulation affecting vertical and meridional atmospheric mixing; (iii) moisture transport pathways in the southern and northern high latitudes; and (iv) ice core stable water isotope composition (δ^{18}O). Having identified significant climate signals at both sites, we test whether constructing a composite series, using ^{10}Be records from both Antarctica and Greenland, is effective in reducing the climate signals and enhancing the solar/production signal.

Finally, following Steig et al. (1996) and Moraal et al. (2005) we use the amplitudes of the 11-yr solar cycles in the ^{10}Be records to constrain the atmospheric source regions of ^{10}Be deposited to the ice sheets.

2. Materials and methods

The DSS ^{10}Be record was sampled from the top 66.62 m of the DSS0506 core, drilled at 66°46.33′S 112°48.43′E, elevation 1370 m asl. The Das2 record was sampled from the 84 m Das2 core, drilled at 67°31.64′N, 36°03.69′W, elevation 2936 m. Dating of the cores and derivation of annual accumulation rates followed previous methods (Palmer et al., 2001; Hanna et al., 2006; van Ommen and Morgan, 2010, for additional details see Supplementary methods). The DSS record spans 1936–2009 and the Das2 record spans 1936–2002. Each ^{10}Be sample integrates deposition over a complete year. The sampling was conducted in a way that reduces the potential for aliasing by seasonal cycles in ^{10}Be concentrations (see Supplementary methods).

^{10}Be measurements were conducted following previous methods at the ANTARES AMS facility, ANSTO, Australia (Fink and Smith, 2007; Pedro et al., 2011a; Simon et al., in press). Measurements were normalised to the National Institute of Standards and Technology USA ^{10}Be standard reference material SRM-4325, utilising the Nishiizumi et al. (2007) ^{10}Be:^{9}Be ratio of $(2.79 \pm 0.02) \times 10^{-11}$. Standard errors in ^{10}Be concentrations (comprising random and systematic measurement errors) ranged from 2.0% to 5.8% with a median of 2.9% for DSS and 1.4–3.5% with a median of 2.6% for Das2. Chemistry procedural blanks gave ^{10}Be:^{9}Be ratios of $< 5 \times 10^{-15}$ and corresponding corrections (typically $< 1-2\%$) were applied to the ^{10}Be measurements.

Atmospheric production rates were calculated using the CRAC:10Be model (Kovaltsov and Usoskin, 2010) and annual average values of the solar modulation constant (Φ). The Φ record is based on neutron monitor counting rates from 1951 to 2010 (adopted from Usoskin et al., 2011) and on the group sunspot number before 1951 (adopted from Usoskin et al., 2002; Vieira et al., 2011). Unless specified the pre-1951 production data is not used here in quantitative analysis as it is less reliable than that from the neutron monitor era. The influence of changes in the strength and configuration of the geomagnetic field on production rates are small on annual to decadal timescales (see e.g. Muscheler et al., 2007b) and are not considered here. We report annual average production rates that are vertically integrated over the entire atmospheric column and averaged over all latitudes (hereafter 'global production rates'), and also columnar production rates averaged over only the geographical latitude range 60–90°S/N, (hereafter 'polar production rates'). Note that other recent models of ^{10}Be production (e.g. Masarik and Beer, 2009) yield production rates that are 30–40% lower than CRAC:10Be. However, for the purpose of this study the absolute production rate is not consequential. Rather, the important detail is the relative production variation during the neutron monitor era, and on this the models are in reasonable agreement (demonstrated in Section 3.3).

Pearson's correlation coefficient (r_{xy}) is used to quantify the degree of (linear) correlation between the ^{10}Be series and production or climate related variables. In calculating correlation coefficients we first linearly detrend all data to reduce the risk of spurious correlations and then employ a non-parametric stationary bootstrap (following Mudelsee, 2003). This approach is preferred over conventional techniques as it yields robust results when applied to autocorrelated, non-normally distributed and unevenly spaced data. The statistical accuracy of correlation coefficients are reported throughout in terms of their 95% confidence intervals (CI), of type bias corrected and accelerated. If the CI contains zero then the correlation is not significant at 95%.

3. Results

3.1. Production and climate signals in ^{10}Be at DSS and Das2

The average annual ^{10}Be concentrations ($\pm 1\sigma$) are $6.07 \pm 1.33 \times 10^3$ atoms g^{-1} in the DSS record (1936–2009) and $5.91 \pm 1.25 \times 10^3$ atoms g^{-1} in the Das2 record (1936–2002). Average annual accumulation rates at the two sites over the same periods are 0.71 ± 0.14 m ice yr^{-1} at DSS and 0.90 ± 0.19 m ice yr^{-1} at Das2. Mean annual ^{10}Be fluxes, calculated from these values (as the product of the respective concentration and accumulation terms) are 125 ± 34 atoms m^{-2} s^{-1} at DSS and 151 ± 30 atoms m^{-2} s^{-1} at Das2.

Time series of the annual variations in average ^{10}Be concentration, accumulation rate and ^{10}Be flux at each site are shown in Fig. 2. The dashed lines mark the annually resolved data and the solid lines show the data smoothed with a Gaussian filter of standard deviation 0.91 yr (equivalent half-power bandwidth to a 3-yr running mean).

Correlation coefficients calculated between the ^{10}Be series and production or climate related variables are listed in Table 1 and are considered in turn below. Unless specified otherwise, the correlation coefficients are determined without applying any time-offset (lag) between the respective series (see Section 3.3 for a discussion of atmospheric residence times).

3.1.1. Cosmic ray intensity and the atmospheric production rate

Average annual polar neutron monitor counting rates (from Usoskin et al., 2005) are shown for 1951–2007 in Fig. 3A. The 11-yr Schwabe cycle modulation of cosmic ray intensity is clearly observed in the neutron data. The alternating peaked and flat topped structure of the 11-yr cycle results from the 22-yr Hale cycle of solar magnetic polarity (see e.g. Webber and Lockwood, 1988).

^{10}Be can be viewed in a sense as a natural neutron monitor (Beer et al., 2011). The agreement between the DSS ^{10}Be concentrations and the cosmic ray intensity (Fig. 3A and B) is visually quite impressive, with the marked exception of their opposing trends during the 1980's. We have no evidence to suggest that this 'missing cycle' in ^{10}Be is associated with our experimental setup or measurement system, rather it is argued (in Section 3.1.3) that it can be linked to climate effects. The Hale cycle reversals of magnetic polarity are not resolved in the ^{10}Be series. Quantitatively, the correlation between DSS concentrations and cosmic ray intensity is significant and of moderate strength, $r_{xy} = 0.54$ with 95% CI [0.31; 0.70] (hereafter expressed in the form $r_{xy} = 0.54[0.31; 0.70]$). For DSS fluxes the agreement with cosmic ray intensity is visually weaker (Fig. 3A and C) and the correlation coefficient is lower, $r_{xy} = 0.38[0.13; 0.57]$.

For Das2 the correlations between cosmic ray intensity and observed concentrations and fluxes (Fig. 3A, D and E) are, respectively, $r_{xy} = 0.45[0.22; 0.62]$ and $r_{xy} = 0.38[0.15; 0.57]$. A marked feature in the Das2 concentrations is the maximum in the 1960s. While this maximum is consistent with the phase of the solar cycle, it greatly exceeds all other decadal signals. Notably, it is substantially reduced in the derived fluxes due to a corresponding pronounced minimum in the Das2 accumulation rate (Fig. 2, right panel).

The CRAC:10Be-modeled global production rates of ^{10}Be are overlain on the DSS and Das2 concentration and flux series in Fig. 3B–E. Solid (grey) lines mark the production rates derived from neutron monitor data while dashed lines mark the less certain production rates pre-1951. An advantage of considering production rates over the neutron monitor record of cosmic ray intensity is that the relative amplitudes of the production and ^{10}Be variations can be quantitatively compared (Section 3.3). Also,

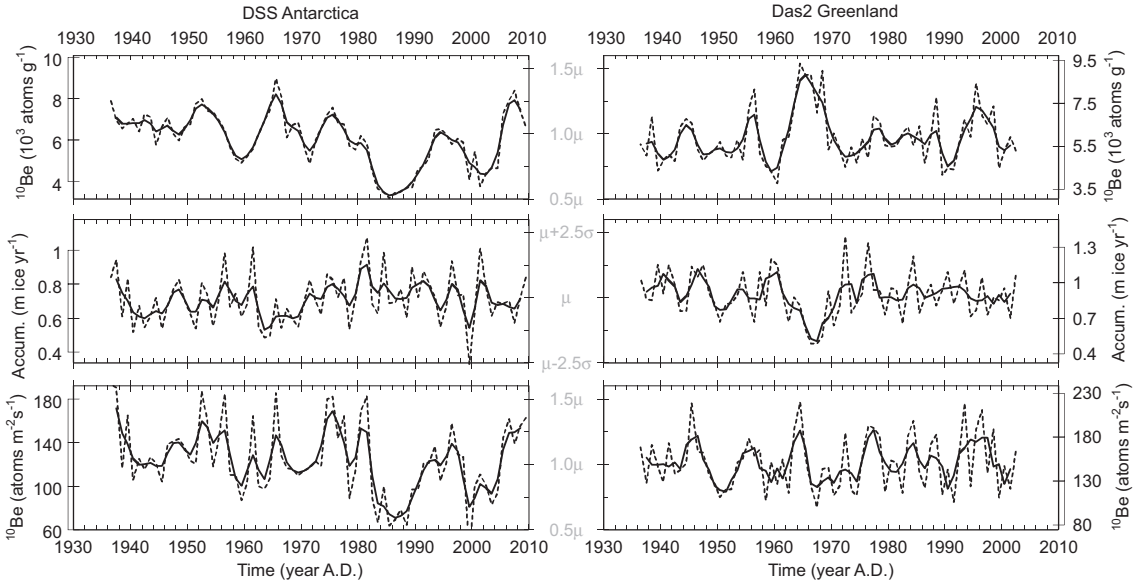

Fig. 2. ^{10}Be concentrations (top), accumulation rates (middle) and ^{10}Be fluxes (bottom) measured in the DSS Antarctica and Das2 Greenland ice cores over recent decades. The vertical axes for concentrations and fluxes are scaled according to the mean (μ) of each record while the vertical axis for accumulation is scaled by the standard deviation (σ) for each record (as can be seen by the internal grey axes). Uncertainties in measured ^{10}Be concentrations are $\sim 3\%$. The dashed lines show annually resolved data and the solid lines show smoothed data (Gaussian filter, effective half-width 3 yr).

Table 1
Testing for significant production and climate signals in the DSS Antarctica and Das2 Greenland ^{10}Be concentration and flux series. Pearson's correlation coefficient r_{xy} is determined between the ^{10}Be series and a suite of production and climate-related parameters, associated 95% confidence intervals are provided in parentheses. Where r_{xy} is shown in bold font the null-hypothesis of no significant relationship can be rejected (as $r_{xy} \neq 0$ at the 95% confidence level). The analysis employs the non-parametric stationary bootstrap (Section 2).

x	Time span	n	$^{10}Be_{Conc}$		$^{10}Be_{Flux}$	
			r_{xy}	[95% CI]	r_{xy}	[95% CI]
DSS Antarctica						
Production parameters						
Neut. count.	1951–2007	57	**0.54**	[0.31; 0.70]	**0.38**	[0.13; 0.57]
Glob. prod.	1951–2009	59	**0.58**	[0.36; 0.73]	**0.39**	[0.14; 0.58]
Glob. prod.	1936–2009	74	**0.54**	[0.33; 0.68]	**0.32**	[0.08; 0.49]
Snow accumulation rate						
Accum.	1936–2009	74	−0.15	[−0.34; 0.07]	**0.62**	[0.45; 0.76]
Modes of atmospheric circulation						
ENSO SOI	1951–2009	59	0.06	[−0.21; 0.32]	0.13	[−0.18; 0.38]
SAM	1979–2009	31	−0.11	[−0.51; 0.28]	−0.26	[−0.60; 0.08]
ZW3	1958–2005	48	**−0.36**	[−0.57; −0.10]	−0.22	[−0.51; 0.13]
DSS ice core parameters						
δ^{18}O	1936–2009	74	−0.17	[−0.39; 0.09]	0.15	[0.09; 0.38]
Das2 Greenland						
Production parameters						
Neut. count.	1951–2002	52	**0.45**	[0.22; 0.62]	**0.38**	[0.15; 0.57]
Glob. prod.	1951–2002	52	**0.44**	[0.19; 0.63]	**0.36**	[0.12; 0.55]
Glob. prod.	1936–2002	67	**0.45**	[0.25; 0.62]	**0.38**	[0.17; 0.54]
Snow accumulation rate						
Accum.	1936–2002	66	**−0.53**	[−0.67; −0.36]	**0.53**	[0.34; 0.67]
Modes of atmospheric circulation						
NAO	1950–2002	53	**−0.42**	[−0.64; −0.15]	−0.13	[−0.37; 0.12]
Das2 ice core parameters						
δ^{18}O	1936–2002	66	−0.05	[−0.27; 0.21]	0.16	[−0.15; 0.36]

Time spans are inclusive. Climate modes from the National Center for Environmental Prediction.
ENSO: http://www.cpc.ncep.noaa.gov/data/indices/soi.
SAM: http://www.cpc.ncep.noaa.gov/products/precip/CWlink/daily_ao_index/aao/.
NAO: ftp://ftp.cpc.ncep.noaa.gov/wd52dg/data/indices/tele_index.nh.

^{10}Be production rates are more sensitive to low energy cosmic rays than are neutron monitors and this is accounted for in the production model. Nevertheless, the correlations between the global production rates and the DSS and Das2 ^{10}Be data are statistically indistinct from those calculated above using cosmic ray intensities, this also applies when the correlation interval is extended to include the less-certain production rates between 1936 and 1951 (see Table 1).

There is a systematic pattern of higher correlations of cosmic ray intensity and calculated production rates with ^{10}Be concentrations than with ^{10}Be fluxes: the coefficients of determination (r^2_{xy}) suggest that, respectively, $\sim$30% and $\sim$20% of the annual variance in ^{10}Be concentrations at DSS and Das2 can be predicted from the cosmic ray intensity data or from modeled production rates, compared to $\sim$15% for flux at both sites. An earlier study (Pedro et al., 2011a), utilising only the most recent 10-yr of the DSS ^{10}Be record, suggested a somewhat stronger production signal in concentrations (controlling $\sim$40% of the variance). As the present result is based on a much longer record it must be considered more robust. The stronger production signals in concentrations compared to fluxes at both DSS and Das2 may be explained in terms of ^{10}Be deposition mechanisms to the sites. Prior observations (Smith et al., 2000; Pedro et al., 2006), and general circulation model (GCM) studies (Pedro et al., 2011b) establish that ^{10}Be is primarily ($>$90%) wet deposited to DSS, i.e. the air to snow transfer takes place with an associated water transfer. GCM studies also suggest that wet deposition of ^{10}Be is dominant at the Das2 site (Field et al., 2006; Heikkilä et al., 2009), although direct observational evidence is lacking. For wet deposition sites the theory of particle deposition to ice sheets advises that the *atmospheric concentration* of a given particulate or aerosol species is more closely related to the species concentration in the ice core than it is to the species inferred flux to the ice core site (the inverse is true for dry deposition sites where atmospheric concentrations are more closely related to flux) (Alley et al., 1995; Davidson et al., 1996). Hence the stronger observed production signal in ^{10}Be concentrations compared to fluxes is in line with the theory.

3.1.2. Accumulation rate

For DSS, the correlation between accumulation rate and ^{10}Be concentration is weak and non-significant, $r_{xy} = -0.15[-0.34; 0.07]$. However, a strong and significant positive correlation is observed between DSS flux and accumulation rate, $r_{xy} = 0.62[0.45; 0.76]$. These results are again consistent with theory (Alley et al., 1995; Davidson et al., 1996): concentrations should be effectively independent of the local accumulation rate at a wet deposition site, as observed; hence calculation of fluxes (by multiplying concentrations by accumulation rate) forces an effectively spurious positive correlation with accumulation rate. In contrast, for a purely dry deposition site, little to no correlation of ^{10}Be flux with accumulation rate would be expected.

Interestingly, there is a significant negative correlation between concentration and accumulation rates at Das2, $r_{xy} = -0.53$ [−0.67; −0.36]. The accumulation signal is not removed by calculating fluxes, $r_{xy} = 0.53[0.34; 0.67]$. The relationship between concentration and accumulation, in a direction that suggests dry deposition, is surprising given the sites near-coastal location and exceptionally high accumulation rate. While an important role for dry deposition cannot be ruled out, we propose an alternative explanation relating to aerosol scavenging during wet deposition. Wet deposition occurs via both in-cloud processes, in which aerosol particles serve as cloud condensation nuclei or ice nuclei ('rainout'), and below cloud processes, through collision of particles with precipitation ('washout') (Davidson et al., 1996). Washout and rainout strip beryllium

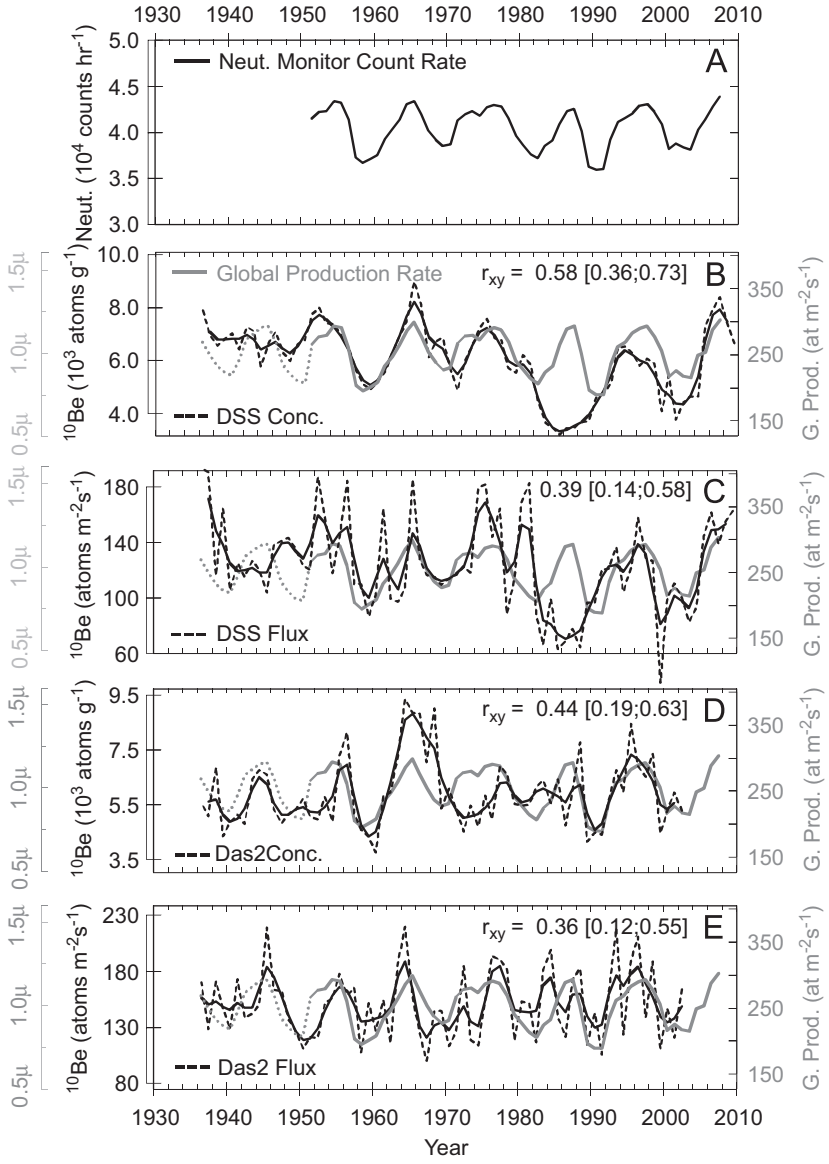

Fig. 3. ^{10}Be concentrations and ^{10}Be fluxes at DSS Antarctica and Das2 Greenland are compared with parameters relating to cosmogenic production rates in the atmosphere. (A) An index of the polar neutron monitor counting rate (from Usoskin et al., 2005). (B–E) The CRAC:10Be-modeled annual average columnar production rate of ^{10}Be in the global atmosphere (solid grey lines) is overlain on the ^{10}Be concentration and flux curves from both sites. The modeled production rates prior to the neutron monitor era (pre-1951, dashed grey lines) are less reliable (Section 2). The axes marking ^{10}Be concentrations and global production rates are scaled according to the mean (μ) of each record (as depicted by the offset grey axes). The dashed lines show annually resolved data and the solid lines show smoothed data (Gaussian filter, effective half-width 3 yr).

radionuclides from the lower troposphere such that their concentration in the air and in the precipitation itself is progressively depleted over the duration of the precipitation event (Brown et al., 1989; Ishikawa et al., 1995). Results from air sampling studies demonstrate that these forms of air mass cleansing occur both at a sampling site and within the moisture transport pathways to it (Feeley et al., 1989). Hence, for the very high accumulation Das2 site, we suggest that the initial stages of large precipitation events may cleanse the atmosphere of its aerosol load while the later stages dilute the impurity in the snowpack. This would be consistent with the observed negative correlation and appears more plausible than a major contribution of dry deposition at such a high-accumulation site.

3.1.3. *Modes of atmospheric circulation*

The DSS concentration and flux data are tested against three major modes of atmospheric variability affecting the southern high latitudes: the El Ninõ Southern Oscillation Index (SOI; 1951–present); the Southern Annular Mode (SAM; 1979–present) and the zonal wave three (ZW3; 1958–present). The SOI affects an array of climate parameters in the Antarctic region (Turner, 2004) and an SOI signal has previously been observed in the shorter-lived cosmogenic ^{7}Be isotope ($t_{1/2} = 53.2$ days) in records from lower latitude air sampling stations (Koch and Rind, 1998). SAM and ZW3 are reported to affect ice core trace chemical composition (Goodwin et al., 2004) and accumulation rates at DSS (van Ommen and Morgan, 2010) through their influence on atmospheric circulation patterns. For the Das2 series we focus on the North Atlantic Oscillation. The NAO affects precipitation rates (e.g. Appenzeller et al., 1998; Vinther et al., 2003), atmospheric transport pathways (e.g. Mosley-Thompson et al., 2005; Sjolte et al., 2011), and stratosphere to troposphere exchange (Baldwin et al., 2001) in the region. An NAO signal in atmospheric ^{10}Be and ^{7}Be data from the northern high-latitudes has previously been reported (Aldahan et al., 2008).

The strengths of the correlations between the ^{10}Be series and respective modes are listed in Table 1. DSS ^{10}Be concentrations are significantly negatively correlated with the ZW3, $r_{xy} = -0.36[-0.57; -0.10]$. However, the correlation is weaker and non-significant with DSS fluxes. No relationship is detected with SAM or ENSO. In the north, Das2 ^{10}Be concentrations are significantly correlated with the NAO index, $r_{xy} = -0.42[-0.64; -0.15]$, and again the correlation with Das2 fluxes is non-significant. These relationships are illustrated in Fig. 4A and B and discussed in turn below.

By definition, a positive ZW3 index indicates strong meridional flow, whereas a negative index indicates weaker meridional and stronger zonal flow (Raphael, 2004). A marked transition in the index from a dominant negative phase toward positive phases occurs in the 1980s (Raphael, 2007). This transition occurs close to the time of the shift toward lower ^{10}Be concentrations through the 1980–1990s. Interestingly, the missing cycle in ^{10}Be falls within the most strongly positive phase of ZW3, Fig. 4A (note the reversed vertical axis). There also appears to be similar periodicity between ZW3 and ^{10}Be in the 1960s and 1970s. Note that the ZW3 index is not itself correlated with cosmic ray intensity ($r_{xy} = -0.14[-0.39; 0.16]$).

A physical explanation for this relationship may be offered by the observed influence of ZW3 on atmospheric transport and regional trends in precipitation rates. During the strong positive phase of ZW3 the large scale atmospheric circulation is characterised by alternating regions of poleward transport of warm mid-latitude air and equatorward transport of cold polar air centered at around 50°S (see Fig. 1 of Raphael, 2004). One of the regions of preferred poleward flow is directed toward Law Dome. National Center for Environmental Prediction (NCEP) reanalysis fields depict increased precipitation in this region of warm moist flow during the positive phase (see Figs. S2 and S4 of van Ommen and Morgan, 2010). We propose that the increased precipitation depletes the air mass aerosol through increased rainout and washout upstream of the DSS site. A similar effect is already observed on intra-annual timescales at Law Dome where consistently low concentrations in the austral winter are linked to the timing of the regional precipitation maximum (Pedro et al., 2011b). Numerous previous studies also observe lower radionuclide concentrations in precipitation following intervals of enhanced precipitation in the moisture transport pathways to precipitation sites (Feeley et al., 1989; Aldahan et al., 2001; Graham et al., 2003; Jordan et al., 2003). By contrast, during the negative phase of ZW3 less cleansing of air masses upstream of the site by precipitation would be expected.

At Das2, Fig. 4B, there is a major shift toward a more positive phase of the NAO after the 1960s (e.g. Scaife et al., 2005), after which similarities are seen in the two time series on both annual and decadal timescales. The ^{10}Be maximum in the mid 1960's occurs during a strong negative phase of NAO, however the two records diverge in the 1950s. Previous studies have argued that a solar activity signal is present in NAO (Lockwood et al., 2010, and references therein). However, for the period under consideration no significant correlation is detected between NAO and cosmic ray intensity, $r_{xy} = -0.16[-0.44; 0.13]$. The lack of correlation remains when a 1 yr lag is introduced to account for time delays (Mavromichalaki et al., 2007) between solar activity changes and changes in cosmic ray intensity, $r_{xy} = -0.08[-0.38; 0.22]$.

A potential explanation for the NAO signal in Das2 concentrations is that moisture transport pathways are more conducive to delivering higher concentrations of ^{10}Be during the negative phase (NAO−), and lower concentrations during the positive phase (NAO+). Baldwin and Dunkerton (2001) observed *reduced* penetration of stratospheric/upper tropospheric air mass (which has high ^{10}Be concentration, Jordan et al., 2003) into the lower levels of the troposphere during NAO+. Similarly, Aldahan et al. (2008) remarked on the absence of stratospheric intrusions in beryllium radionuclide data from two high latitude sites in Sweden during the strong NAO+ between 1989 and 1992. In addition, evidence from Lagrangian-based moisture transport diagnostics suggest that moisture transport pathways to central-eastern Greenland are typically longer during NAO− (Sodemann et al., 2008), thus increasing the range for aerosol scavenging, which is also consistent with the higher observed concentrations during NAO−.

The important role of NAO in precipitation rate variability in the region should also be considered (see e.g. Appenzeller et al., 1998; Vinther et al., 2003; Mosley-Thompson et al., 2005; Hanna et al., 2006). Using data from the ECMWF ERA-15 reanalysis, Appenzeller et al. (1998) demonstrated that the precipitation response to NAO has pronounced spatial variability (see their Fig. 1B): on the western-central side of Greenland precipitation rates are significantly negatively correlated with the NAO, whereas on the eastern-central side (where Das2 is located) precipitation rates are significantly positively correlated with

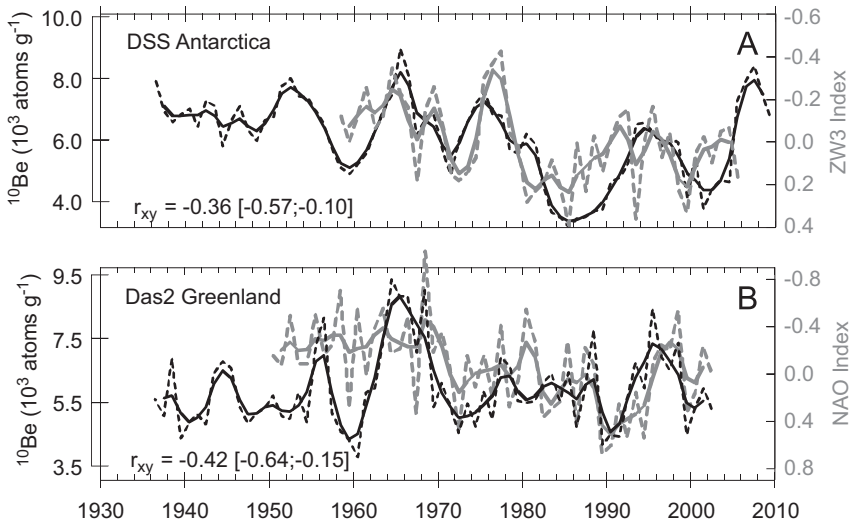

Fig. 4. ^{10}Be concentrations are compared with modes of atmospheric circulation. (A) The southern hemisphere zonal wave three (ZW3) index at the 500 mb level (annual averages from Raphael, 2004) overlain on ^{10}Be concentrations at DSS Antarctica. (B) The North Atlantic Oscillation (NAO) index (annual averages from the National Center for Environmental Prediction) is overlain on ^{10}Be concentrations from Das2 Greenland. Both indices are shown on inverted axes. The dashed lines show annually resolved data and the solid lines show smoothed data (Gaussian filter, effective half-width 3 yr).

the NAO. This pattern is also seen in a recent meso-scale model study (Sjolte et al., 2011). In line with these studies, the accumulation rate at Das2 is positively correlated with the NAO, $r_{xy}=0.29$, although the significance is marginal, 95% CI [−0.03; 0.54] (Supplementary Fig. S1). The fact that the relationship between ^{10}Be concentrations and NAO is stronger than the relationship between accumulation rate and NAO suggests that this is not entirely an accumulation-driven effect. To summarise, we suggest that the directions of the observed correlations are consistent with two contributing factors: (i) NAO controls on atmospheric transport processes including stratosphere to troposphere exchange and (ii) NAO modulation of accumulation rate at the Das2 site and in the moisture transport pathways to it, causing depletion of ^{10}Be concentrations in precipitation via washout and rainout during the higher precipitation NAO+ phase.

3.1.4. δ^{18}O

Results from an earlier sub-monthly resolved snow pit study at the DSS site found a strong and significant negative correlation between δ^{18}O ratios and ^{10}Be concentrations on sub-monthly timescales (Pedro et al., 2006). Higher (warmer) δ^{18}O values, which are typically associated with enhanced influence of warm and moist marine air, coincided with reduced ^{10}Be concentrations; whereas, lower (colder) δ^{18}O values, which are typically associated with enhanced influence of continental air, coincided with higher ^{10}Be concentrations. A negative correlation is also observed here in the annually resolved DSS concentrations, however it is weaker than that observed previously and it marginally fails a significance test $r_{xy}=-0.17[-0.39;0.09]$. No correlation is apparent between Das2 concentrations and δ^{18}O. Overall it appears that the effect identified in Pedro et al. (2006) is strong on the snowfall event scale but relatively weak when considered on annual timescales. The weakening of the relationship in more coarsely resolved data is in line with other recent work at the site (Pedro et al., 2011a), and suggests that some local climate signals are reduced simply by averaging data over longer time periods.

3.2. A bipolar ^{10}Be composite record

The preceding sections demonstrate that, on annual timescales, the ^{10}Be records from DSS and Das2 contain both production and climate signals of comparable strengths. In the context of using ^{10}Be as a solar proxy, we would like to enhance the production signal and reduce the climate 'noise'. A simple yet powerful technique for enhancing the signal to noise ratio in precisely dated ice cores is to make a composite or stack of multiple records (e.g. Fisher et al., 1996; Delaygue and Bard, 2011). The technique rests on the assumption that the signal, in this case the atmospheric production rate, is common and will be reinforced. In Fig. 5, the DSS and Das2 records are shown together with other annually resolved ^{10}Be records from the neutron monitor era: those from the Greenland sites, North GRIP (Berggren et al., 2009), Dye 3 (Beer et al., 1984) and Renland (Aldahan et al., 1998) and the Antarctic site, Dronning Maud Land (Aldahan et al., 1998); for core locations see Fig. 1. We use the timescales reported by the original authors, all determined by annual layer counting.

The time series of concentrations from each site are normalised separately by dividing by their respective means over the period 1951–1984 (this period is selected as it is common to all records). Each series is overlain with the global ^{10}Be production rate, which is normalised in the same way (the issue of global versus polar mixing is addressed in the next section). The correlation coefficients and associated 95% CIs between each ^{10}Be series and the global production rate are inset on each plot.

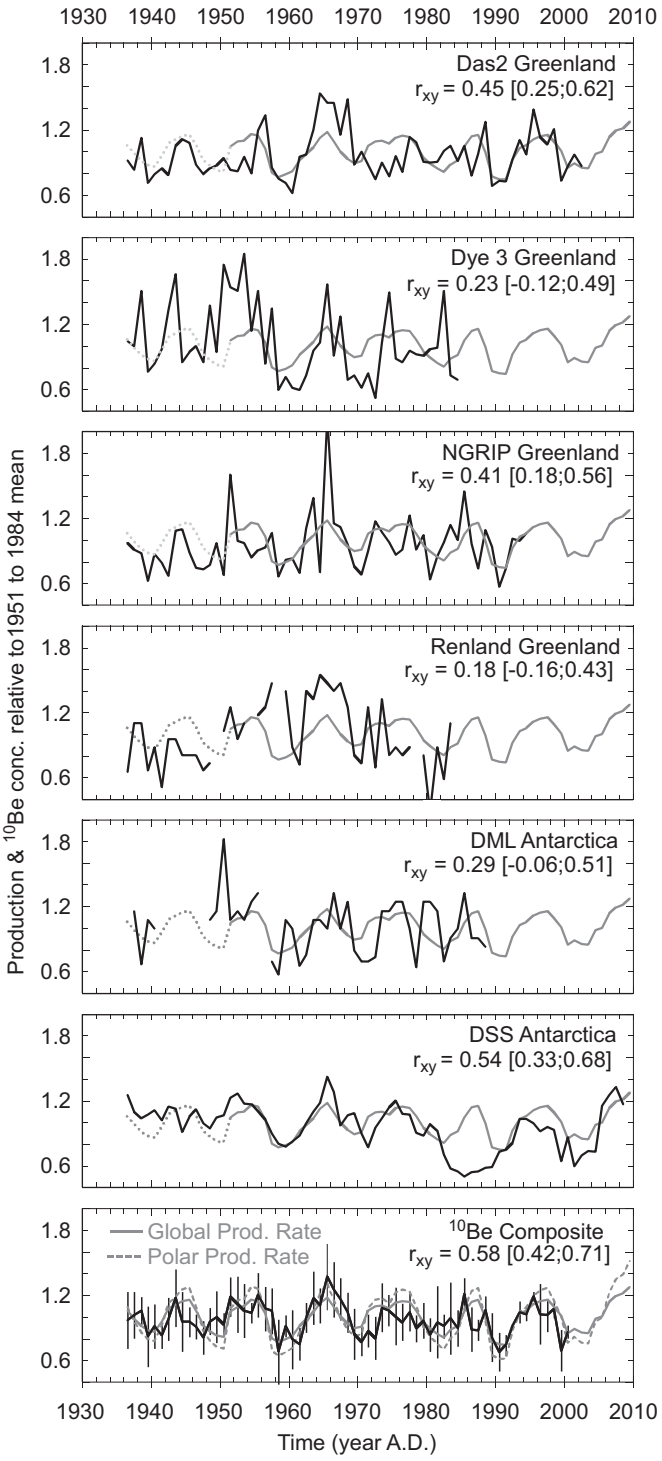

Fig. 5. ^{10}Be records from Antarctic and Greenland sites during the neutron monitor era. Each record is overlain with the CRAC:10Be-modeled global ^{10}Be production rate. The bottom panel shows a composite record constructed by stacking all of the records from the individual sites (see Section 3.2). The error bars on the composite curve show the standard deviation of the composite members at each time step. Global average and polar average ^{10}Be production rate curves are both overlain on the ^{10}Be composite. All axes are scaled according to the mean values (μ) of the individual records over the common interval 1951–1984. Note that the production rates prior to 1951 are less reliable (Section 2). Data sources, Dye 3 (Beer et al., 1984), NGRIP (Berggren et al., 2009) and Renland and Dronning Maud Land (DML; Aldahan et al., 1998).

Among the individual sites, DSS has the highest correlation, followed by Das2. The attention paid here to sampling the DSS and Das2 records in a way that reduces seasonal aliasing may

have contributed to their higher correlations (see Supplementary Methods). Among the remaining sites North-GRIP is most strongly correlated, whilst the correlations at Dye 3, Renland and DML are positive but not significantly different from zero. The weaker correlations at the later sites may be partly associated with their relatively high measurement uncertainties (10–15%) (Beer et al., 1984; Aldahan et al., 1998), compared to uncertainties of $<5\%$ in the more recently measured DSS, Das2 and NGRIP records (Section 2; Berggren et al., 2009).

The lowermost panel of Fig. 5 shows the average or composite of all six evenly weighted normalised records. The composite is limited to the period 1936–2002, during which there are at least two records available for averaging. In constructing the composite, annual concentrations that were more than two standard deviations away from the mean of the respective record were excluded. This form of filtering is justified by prior work linking such signals to meteorological variability, in particular stratosphere to troposphere exchange events (Aldahan et al., 2008; Pedro et al., 2011b).

The composite is more strongly correlated to the global production rate, $r_{xy}=0.62[0.43;\ 0.75]$, and the cosmic ray intensity, $r_{xy}=0.61[0.44;\ 0.74]$, than any of the individual cores (see Table 2 and Fig. 5). Furthermore, the composite is not correlated to the atmospheric modes identified earlier. For example the correlation between the composite and NAO is $r_{xy}=-0.05[-0.31;\ 0.27]$, and between the composite and ZW3 is $r_{xy}=-0.10[-0.34;\ 0.14]$. This illustrates that the signal to noise ratio has indeed been increased.

Spectral analysis provides additional insight into the production signal in the ^{10}Be composite. Fig. 6 compares the power spectrum of the ^{10}Be composite to that of the atmospheric production rate and the individual DSS and Das2 records (for computation of the power spectrum see Supplementary methods). The solar-cycle is clearly expressed in production rates as a peak at period 10.8 yr. The ^{10}Be composite captures the period of the solar cycle very well, also showing a peak, albeit somewhat broader, at 10.8 yr. By contrast in the individual cores the period of the solar cycle (at least for the time interval under consideration) is poorly resolved; at DSS power is split between peaks at 10.4 and 14.6 yr and at Das2 in a broad maximum between 9.4 and 16.3 yr. This illustrates that the spectral coherence of the production signal is enhanced in the composite ^{10}Be record compared to in the individual records.

Table 2
Assessing the strength of production signals in the multi-core ^{10}Be composite. Pearson's correlation coefficient, r_{xy}, is determined between the composite and polar neutron monitor counting rates (representing cosmic ray intensity) and the composite and CRAC:10Be-modeled ^{10}Be production rates. All correlations are significant at the 95% confidence level.

x	*Time span*	*n*	r_{xy}	[95% CI]
Production				
Neut. count	1951–2002	52	**0.61**	[0.44 ; 0.74]
Glob. prod.	1951–2002	52	**0.62**	[0.43; 0.75]
Glob. prod.	1936–2002	67	**0.58**	[0.42; 0.71]

3.3. Global or polar mixing of ^{10}Be

Cosmic rays are directed toward the geomagnetic poles leading to production rates over the polar latitudes ($>60^{\circ}$S/N) that are $\sim 3-20$ times greater (depending on altitude) than those over the lower latitudes (Kovaltsov and Usoskin, 2010). More importantly, in the context of interpreting ^{10}Be as a solar activity proxy, the *amplitude* of the solar modulation of production is greater over the polar latitudes than over the lower latitudes. This can be illustrated using the CRAC:10Be production data: throughout the neutron monitor era, the amplitudes of the 11-yr cycles in columnar production variations in the polar atmosphere are on average 1.63 times those averaged over all latitudes (Fig. 5, bottom panel).

The amplitudes of the 11-yr cycles in observed ^{10}Be concentrations can thus be used to examine whether the ^{10}Be deposited to the ice sheets is produced mainly at polar latitudes, or rather represents production in the globally well-mixed atmosphere

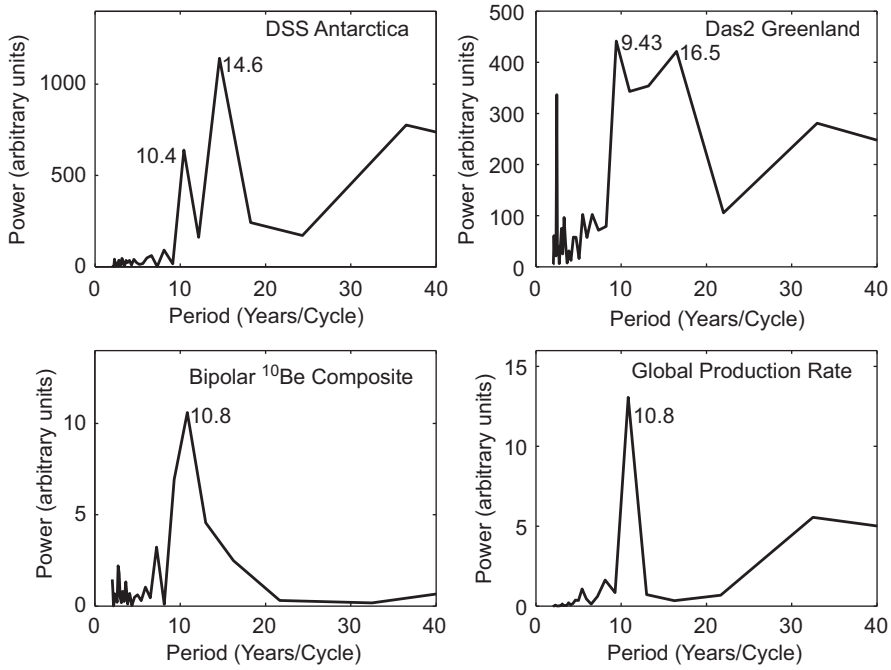

Fig. 6. The Fourier spectrums of the ^{10}Be records from DSS Antarctica (top left) and Das2 Greenland (top right) are compared against the spectrums of the bipolar ^{10}Be composite (bottom left) and the global ^{10}Be production rate (bottom right). The similarity of the composite spectrum to the production rate spectrum suggests that combining multiple ^{10}Be records reduces non-production noise.

(following e.g. Steig et al., 1996; Moraal et al., 2005). Any such analysis should also take into account attenuation of the 11-yr cycle amplitude due to mixing of ^{10}Be during its atmospheric residence time. Following Bard et al. (1987), the level of attenuation (A) can be expressed in terms of the production modulation periodicity (T, which here is 11 yr) and the atmospheric residence time (τ):

$$A = \frac{1}{\sqrt{1+\left(\frac{2\pi\tau}{T}\right)^2}}$$

There is negligible attenuation of the troposphere-produced ^{10}Be during its several-week residence time. However, due to the longer residence time in the stratosphere the stratosphere-produced signal will be significantly affected. The situation is simplified by considering the mean residence time. A lagged-correlation analysis provides a first-order estimate of this parameter, under the assumption that the maximum correlation will be observed at lag $\equiv \tau$. The lagged correlations for DSS, Das2 and the bipolar composite are shown in Fig. 7 with their associated 95% CIs. The correlations are highest at lags of 0–1 yr, somewhat lower at lags of 2 yr and not significantly different from zero at lags of 3 yr. This agrees with an earlier lag-correlation analysis based on quasi-monthly resolved DSS data that suggested a likely residence time of $\sim$10 months or less. Previous estimates based on ^{10}Be:^{7}Be ratios (Raisbeck et al., 1981) and GCM modeling (Heikkilä et al., 2009) also suggest residence times of $\sim$1-yr or less.

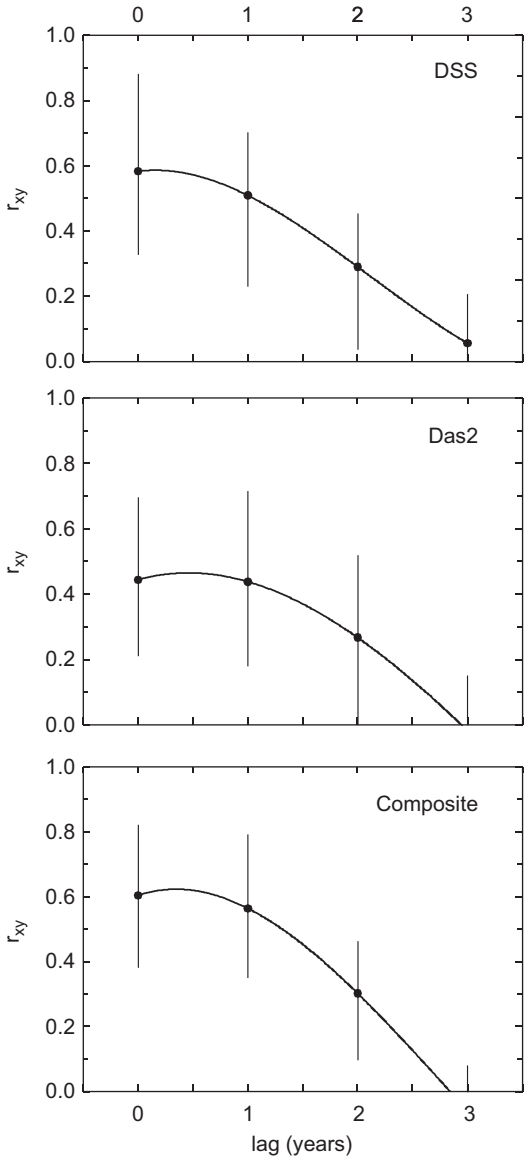

Fig. 7. Time-lagged correlation plots of ^{10}Be concentrations against the CRAC:10Be-modeled global ^{10}Be production rates. DSS (top), Das2 (middle) and the bipolar composite (bottom). Error bars show the 95% CIs around the correlation coefficients. The curves are least squares polynomial fits to the data points.

The ^{10}Be and production data are first normalised as in Section 3.2. Considering separately the DSS, Das2 and composite ^{10}Be records, we use linear regression to quantitatively compare the relative amplitudes of the 11-yr signals in the observed concentrations and the global and polar production rates. The critical regression parameter here is the slope; if the 95% CI around the slope contains 1 then it implies that the relative amplitude of the 11-yr cycles in ^{10}Be and in the production series are not significantly different. The regression parameters are estimated by non-parametric bootstrap resampling with replacement (1000 times) from the available data.

Results are presented in Fig. 8A–F. The regression lines and associated 95% CIs (dashed lines) are plotted on each sub-figure and the slopes (b_1) are listed inset. The scaled slopes, (b_1/A), under the assumption of a 1-yr mean atmospheric residence time ($\tau = 1$, $A = 0.87$) are also listed on the sub-figures. Regression slopes under the assumption of a wider range of residence times ($\tau = 1$, 1.5, 2.0 and 2.5 yr) are listed in Supplementary Table S1. For residence times less than 1.5 yr the 95% CIs around the slopes of the regression against global production are consistent with 1, whereas the slopes of the regression against the polar production rate are significantly < 1. This is consistent with substantial input of ^{10}Be produced at low latitudes and inconsistent with an exclusively polar production source. However, under the assumption of mean residence time of ≥ 2 yr for DSS and Das2 and ≥ 2.5 yr for the composite the method cannot clearly distinguish a dominant source region. A mean residence time in this range cannot be ruled out but would appear unlikely based on the lagged correlation analysis and most though not all (Baroni et al., 2011) previous studies.

Independent evidence supporting substantial meridional mixing of ^{10}Be includes the observed geomagnetic imprints in ^{10}Be records from both Antarctica and Greenland (Mazaud et al., 1994; Wagner et al., 2000; Raisbeck et al., 2006). Whereas, if the ice sheets sampled exclusively ^{10}Be produced at polar latitudes then geomagnetic field changes should not be visible at all. In addition, model output from the ECHAM5-HAM GCM, suggests that at least the stratosphere-produced component of the ^{10}Be observed in polar ice cores is well-mixed meridionally (Heikkilä et al., 2009; Muscheler and Heikkilä, 2011). Simulations with the GISS ModelE GCM also support meridional mixing but suggest a small ($\sim$20%) bias toward polar-produced ^{10}Be (Field et al., 2006).

Opposing views have also been presented. An exclusively polar production source for South Pole ^{10}Be was suggested on the basis of a multi-centenary-scale intercomparison with cosmogenic ^{14}C from tree rings (Bard et al., 1997). This result has been a subject of debate elsewhere (see e.g. Bard et al., 2007; Muscheler et al., 2007a). Also, Steig et al. (1996) support a polar origin for ^{10}Be at Taylor Dome, Antarctica on the basis that the amplitude of the 11-yr cycle at that site significantly *exceeds* global production variations. There are several possible reasons for the difference between our result and that of Steig et al. (1996). (i) Different production models: Steig et al. (1996) calculated ^{10}Be production rates using the O'Brien et al. (1991) production model forced with cosmic ray intensity from the Deep River neutron monitor; whereas here we use the CRAC:10Be production model forced with the Usoskin et al. (2011) Φ reconstruction. (ii) Different time-spans of the records: The Taylor

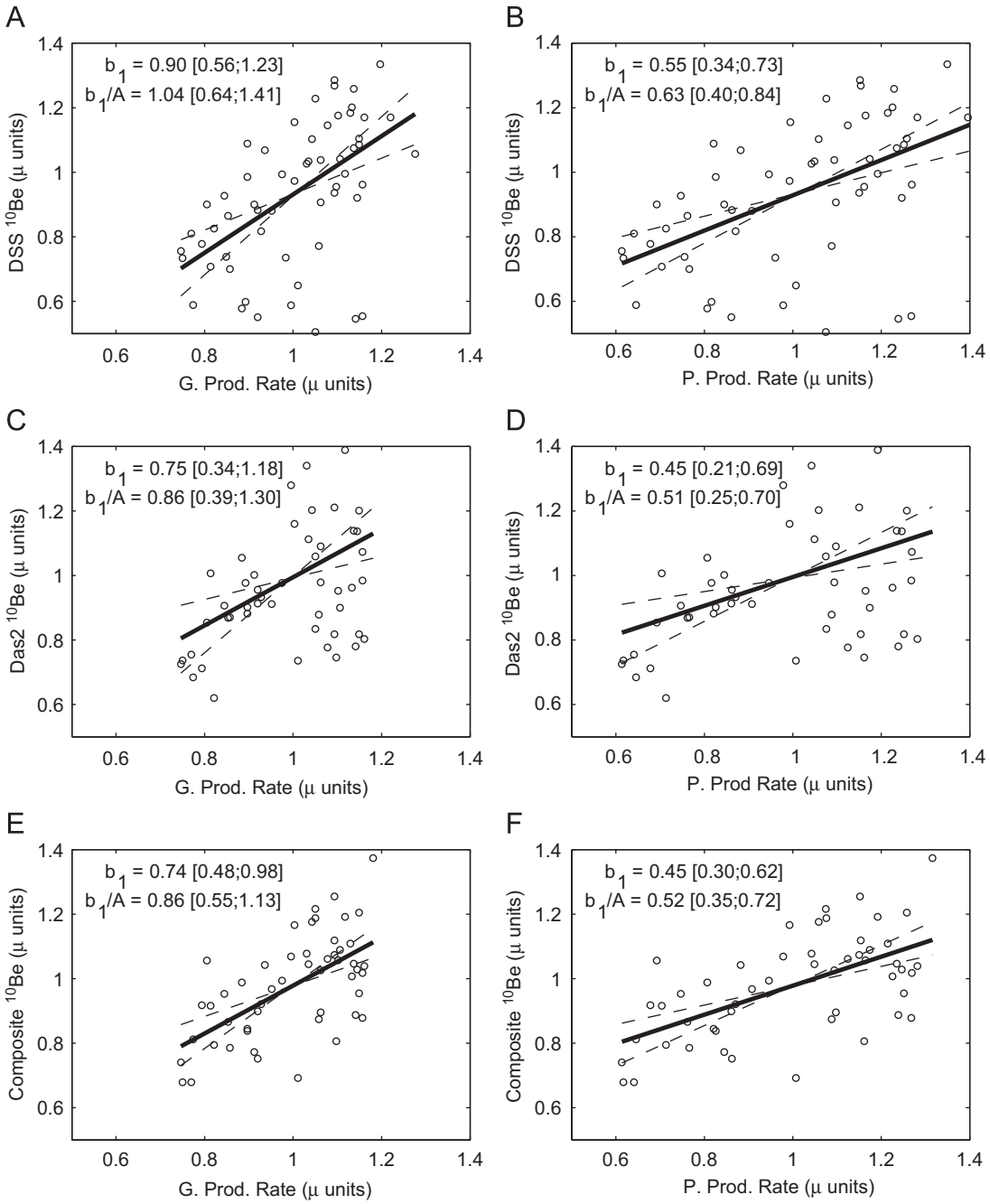

Fig. 8. Evaluating the atmospheric production source regions of the ^{10}Be preserved in the ice core records. The amplitudes of the 11-yr cycles in observed ^{10}Be concentrations are regressed against the global (left) and polar (right) production rates. Results are shown for DSS concentrations (top), Das2 concentrations (middle) and the ^{10}Be composite (bottom). Concentrations and production rates are expressed relative to the mean values (through 1951–1984) of the respective records. Solid lines show the best fit regression lines and the dashed lines show 95% confidence intervals around the regression slopes (b_1), also listed inset with the 95% CI in parentheses. Scaled versions of the regression slopes (b_1/A, where A=0.86) are also provided, these account for the amplitude attenuation that would be expected due to a 1-yr mean atmospheric residence time for ^{10}Be (see text). For all three ^{10}Be records the unscaled and scaled regression slopes against the global columnar production rates are consistent with 1 at 95% confidence, whereas the regressions against polar columnar production rates are significantly less than 1.

Dome study was limited to 37-yr of overlap with production rate data compared to 59-yr at DSS and 52-yr for both Das2 and the ^{10}Be composite. (iii) Different data treatment prior to analysis: the Taylor Dome record was measured at 2–3-yr resolution then resampled to annual resolution using low-degree cubic splines then filtered with a 9–13-yr bandpass filter; whereas the analysis here is performed directly on annually resolved and unfiltered data. To test the sensitivity of our results to point (i) the analysis was repeated using the Masarik and Beer (2009) ^{10}Be production model, forced as for CRAC:10Be, with the Usoskin et al. (2011) Φ reconstruction (Supplementary Fig. S2). The regression slopes are shifted marginally higher under the Masarik and Beer (2009) model, but still favour substantial meridional mixing under the mean residence time assumptions above. With regard to points (ii) and (iii), the longer period of overlap, consistent results for multiple records and use of annually resolved data lend support to our conclusions. It is possible that the higher amplitude observed in the shorter Taylor Dome record may have resulted from the superposition of climate effects on the production signal, for example as appears to have occurred in the Greenland records during the 1960s (Fig. 5).

4. Discussion and conclusions

The DSS and Das2 ^{10}Be records are significantly correlated with cosmic ray intensity and CRAC:10Be atmospheric production rates. The correlations are stronger at DSS than at Das2 and stronger with concentrations than with fluxes. The weaker signal in fluxes advises against using the flux term *at wet deposition sites* as an input for solar activity and cosmic ray intensity reconstructions during the late Holocene. Note that this conclusion does not apply during the last glacial period and deglaciation. The major regional and hemispheric-scale changes in precipitation rates during those periods strongly modulated ^{10}Be concentrations in all records that have so far been recovered (e.g. Raisbeck et al., 1987; Yiou et al., 1997; Wagner et al., 2001).

Significant portions of the variance in the ^{10}Be records are also associated with non-production or climate signals. At DSS concentrations appear to be influenced by the ZW3 pattern of atmospheric circulation. At Das2 concentrations appear to be influenced by the NAO and the local accumulation rate. The sensitivity of the DSS and Das2 records to modes of atmospheric circulation has potential implications for the interpretation of longer term records (spanning centuries to millennia). It suggests that climate signals in ^{10}Be data may include systematic components that would not necessarily be removed by low-pass filtering. This can be illustrated by the NAO and ^{10}Be anti-correlation at Das2. A period of relative warmth in the North Atlantic sector around the 9th–12th century AD, the 'medieval warm period', has been linked to a prolonged positive NAO phase (e.g. Trouet et al., 2009); whereas a period of relative cold in this sector around the 16th–19th century AD, the 'little ice age', has been linked to a prolonged negative NAO phase (Slonosky et al., 2001; Trouet et al., 2009). Our results suggest that the patterns of circulation during these climate events could systematically influence ^{10}Be transport and deposition to some Greenland sites. For the Das2 site the direction of the correlation is such that it would act to exaggerate the proposed high solar activity during the medieval warm period and the low solar activity during the little ice age. It would clearly be advisable to avoid using any records affected in this way as sole inputs to solar reconstructions and solar forcing attribution studies. Given that the influence of NAO on the ice sheet appears to vary spatially (e.g Appenzeller et al., 1998), the problem may affect other sites differently or not at all. Encouragingly, the NGRIP record is uncorrelated, $r_{xy} = -0.03[-0.27;\ 0.22]$, to the NAO at least through the interval 1950–1994. However, suitable data is currently unavailable to test whether this is also the case at GRIP, such a test would be useful as the GRIP record has been widely used in solar reconstructions (Vonmoos et al., 2006; Muscheler et al., 2007b; Shapiro et al., 2011; Steinhilber et al., 2012).

The potential for systematic climate influences on ^{10}Be at some sites advises caution in the interpretation of individual cores and underlines the importance of techniques to enhance the production signal. A bipolar composite record constructed using all available annually resolved ^{10}Be records from the neutron monitor era is more strongly correlated with cosmic ray intensity than any individual record. This suggests that studies which assimilate bipolar composite ^{10}Be records in solar or cosmic ray intensity reconstructions (e.g. Steinhilber et al., 2012), or variants, such as the leading principal component of multiple records (e.g. Muscheler et al., 2007b) are less likely to introduce spurious climate-related signals than those assimilating ^{10}Be records from individual sites (e.g. Bard et al., 2000; Vonmoos et al., 2006; Shapiro et al., 2011). Using multiple ^{10}Be records in addition to cosmogenic ^{14}C (from tree rings), which has a very different geochemical behaviour to ^{10}Be, can help to further decouple the climate signal from the ^{10}Be record (e.g. Muscheler et al., 2007b; Usoskin et al., 2009; Steinhilber et al., 2012).

The amplitudes of the 11-yr signals in the DSS, Das2 and composite records were used to examine the atmospheric source regions of the ^{10}Be deposited to the ice core sites. Under the assumption of a mean atmospheric residence time for ^{10}Be of ≤ 1.5 yr, supported by most previous studies, the 11-yr signal in ^{10}Be is consistent with the amplitude of the CRAC:10Be production variations in the global atmosphere and inconsistent with the amplitude of production variations in the polar atmosphere. Some polar bias in the atmospheric source region for the ice core ^{10}Be is not inconsistent with this finding, but an exclusively polar source would appear unlikely. This is in agreement with the mixing scenarios favoured by most recent ^{10}Be-based solar reconstructions; i.e. that the ice sheets sample ^{10}Be from a relatively well-mixed global atmosphere (Vonmoos et al., 2006; Muscheler et al., 2007b; Steinhilber et al., 2009, 2012).

The data sets are available online at the Australian Antarctic Data Center (http://data.aad.gov.au/) and at the World Data Center for Paleoclimatology (http://www.ncdc.noaa.gov/paleo/).

Acknowledgements

The authors acknowledge support from the Australian Antarctic Division (AAS#2384, AAS#3064 and AAS#1172), the Australian Government's Cooperative Research Centres Programme through the Antarctic Climate & Ecosystems Cooperative Research Centre (ACE CRC) and the Isotopes in Climate Change and Atmospheric Systems (ICCAS) project at the Australian Nuclear Science and Technology Organisation (ANSTO). The NASA Cryosphere program supported the acquisition of the Das2 ice core. Funding for continuous chemical and elemental analyses of the DSS and DAS2 cores at the Desert Research Institute (DRI) was also provided by the NASA Cryosphere program and the Arctic Section of NSF's Office of Polar Programs. The staff and students in the DRI ice core chemistry lab are thanked for their assistance in analysing the ice cores. Illya Usoskin generously provided the CRAC:10Be model data. J.B.P. is grateful for the support of an Australian Institute of Nuclear Science and Engineering (AINSE) Post-Graduate Research Award. Constructive comments from three anonymous reviewers helped to strengthen the manuscript.

Appendix A. Supplementary data

Supplementary data associated with this article can be found in the online version at http://dx.doi.org/10.1016/j.epsl.2012.08.038.

References

Aldahan, A., Hedfors, J., Possnert, G., Kulan, A., Berggren, A.-M., Söderström, C., 2008. Atmospheric impact on beryllium isotopes as solar activity proxy. Geophys. Res. Lett. 35, L21812.

Aldahan, A., Possnert, G., Johnsen, S., Clausen, H., Isaksson, E., Karlen, W., Hansson, M., 1998. Sixty year ^{10}Be record from Greenland and Antarctica. In: Proceedings of the Indian Academy of Sciences (Earth and Planetary Science Letters), vol. 107, pp. 139–147.

Aldahan, A., Possnert, G., Vintersved, I., 2001. Atmospheric interactions at northern high latitudes from weekly Be-isotopes in surface air. Appl. Radiat. Isotopes 54 (2), 345–353.

Alley, R.B., Finkel, R.C., Nishiizumi, K., Anandakrishnan, S., Shuman, C.A., Mershon, G.R., Zielinski, G.A., Mayewski, P.A., 1995. Changes in continental and sea-salt atmospheric loadings in central Greenland during the most recent deglaciation: model-based estimates. J. Glaciol. 41, 503–514.

Ammann, C.M., Joos, F., Schimel, D.S., Otto-Bliesner, B.L., Tomas, R.A., 2007. Solar influence on climate during the past millennium: results from transient simulations with the NCAR climate system model. Proc. Natl. Acad. Sci. U.S.A. 104, 3713–3718.

Appenzeller, C., Schwander, J., Sommer, S., Stocker, T.F., 1998. The north atlantic oscillation and its imprint on precipitation and ice accumulation in Greenland. Geophys. Res. Lett. 25, 1939–1942.

Baldwin, M.P., Dunkerton, T.J., 2001. Stratospheric harbingers of anomalous weather regimes. Science 294, 581–584.

Baldwin, M.P., Gray, L.J., Dunkerton, T.J., Hamilton, K., Haynes, P.H., Randel, W.J., Holton, J.R., Alexander, M.J., Hirota, I., Horinouchi, T., Jones, D.B.A., Kinnersley, J.S., Marquardt, C., Sato, K., Takahashi, M., 2001. The quasi-biennial oscillation. Rev. Geophys. 39, 179–230.

Bard, E., Arnold, M., Duprat, J., Moyes, J., Duplessy, J.-C., 1987. Reconstruction of the last deglaciation: deconvolved records of δ^{18}O profiles, micropaleontological variations and accelerator mass spectrometric ^{14}C dating. Clim. Dyn. 1, 101–112.

Bard, E., Raisbeck, G., Yiou, F., Jouzel, J., 2000. Solar irradiance during the last 1200 years based on cosmogenic nuclides. Tellus B 52, 985–992.

Bard, E., Raisbeck, G.M., Yiou, F., Jouzel, J., 1997. Solar modulation of cosmogenic nuclide production over the last millennium: comparison between ^{14}C and ^{10}Be records. Earth Planet. Sci. Lett. 150, 453–462.

Bard, E., Raisbeck, G.M., Yiou, F., Jouzel, J., 2007. Comment on "Solar activity during the last 1000 yr inferred from radionuclide records" by Muscheler et al. (2007). Quat. Sci. Rev. 26, 2301–2304.

Baroni, M., Bard, E., Petit, J.-R., Magand, O., Bourlès, D., 2011. Volcanic and solar activity, and atmospheric circulation influences on cosmogenic ^{10}Be fallout at Vostok and Concordia (Antarctica) over the last 60 years. Geochim. Cosmochim. Acta 75, 7132–7145.

Beer, J., McCracken, K.G., Abreu, J., Heikkilä, U., Steinhilber, F., 2011. Cosmogenic radionuclides as an extension of the neutron monitor era into the past: potential and limitations. Space Sci. Rev. 322 (December).

Beer, J., Oeschger, H., Andrée, M., Bonani, G., Suter, M., Wölfli, W., Langway Jr., C.C., 1984. Temporal variations in the ^{10}Be concentration levels found in the Dye 3 ice core, Greenland. Ann. Glaciol. 5, 16–17.

Berggren, A., Beer, J., Possnert, G., Aldahan, A., Kubik, P., Christl, M., Johnsen, S.J., Abreu, J., Vinther, B.M., 2009. A 600-year annual ^{10}Be record from the NGRIP ice core, Greenland. Geophys. Res. Lett. 36, L11801.

Brown, L., Stensland, G.J., Klein, J., Middleton, R., 1989. Atmospheric deposition of ^{7}Be and ^{10}Be. Geochim. Cosmochim. Acta 53 (1), 135–142.

Davidson, C.I., Bergin, H., Hampden, D., 1996. The deposition of particles and gasses to ice sheets. In: Wolff, E., Bales, R. (Eds.), NATO ASI Series, Chemical Exchange Between the Atmosphere and Polar Snow, vol. I 43. Springer, pp. 275–306.

Delaygue, G., Bard, E., 2011. An Antarctic view of beryllium-10 and solar activity for the past millennium. Clim. Dyn. 36 (11–12), 2201–2218.

Feeley, H.W., Larsen, R.J., Sanderson, C.G., 1989. Factors that cause seasonal variations in beryllium-7 concentrations in surface air. J. Environ. Radioact. 9, 223–249.

Field, C.V., Schmidt, G.A., 2009. Model-based constraints on interpreting 20th century trends in ice core ^{10}Be. J. Geophys. Res. 114, D12110.

Field, C.V., Schmidt, G.A., Koch, D., Salyk, C., 2006. Modeling production and climate-related impacts on ^{10}Be concentration in ice cores. J. Geophys. Res. 111, D15107.

Fink, D., Smith, A., 2007. An inter-comparison of ^{10}Be and ^{26}Al AMS reference standards and the ^{10}Be half-life. Nuclear Instruments and Methods in Physics Research Section B 259, 600–609.

Fisher, D., Koerner, R.M., Kuivinen, K., Clausen, H.B., Johnsen, S.J., Steffensen, J.-P., Gundestrup, N., Hammer, C.U., 1996. Inter-comparison of δ^{18}O and precipitation records from sites in Canada and Greenland over the last 3500 years and over the last few centuries in detail using EOF techniques. In: Jones, P.D., Bradley, R.S., Jouzel, J. (Eds.), Climatic Variations and Forcing Mechanisms of the Last 2000 Years, ASI Series 1: Global Environmental Change, vol. 41. Springer, pp. 297–328.

Goodwin, I.D., van Ommen, T.D., Curran, M.A.J., Mayewski, P.A., 2004. Mid latitude winter climate variability in the South Indian and southwest Pacific regions since 1300 AD. Clim. Dyn. 22, 783–794.

Graham, I., Ditchburn, R., Barry, B., 2003. Atmospheric deposition of ^{7}Be and ^{10}Be in New Zealand rain. Geochim. Cosmochim. Acta 67, 361–373.

Hanna, E., McConnell, J., Das, S., Cappelen, J., Stephens, A., 2006. Observed and modeled Greenland Ice Sheet snow accumulation, 1958–2003, and links with regional climate forcing. J. Clim. 19, 344–358.

Heikkilä, U., Beer, J., Feichter, J., 2009. Meridional transport and deposition of atmospheric ^{10}Be. Atmos. Chem. Phys. 9, 515–527.

Igarashi, Y., Hirose, K., Otsuji-Hatori, M., 1998. Beryllium-7 deposition and its relation to sulfate deposition. J. Atmos. Chem. 29, 217–231.

Ishikawa, Y., Murakami, H., Sekine, T., Yoshihara, K., 1995. Precipitation scavenging studies of radionuclides in air using cosmogenic ^{7}Be. J. Environ. Radioact. 26 (1), 19–36.

Jordan, C.E., Dibb, J.E., Finkel, R.C., 2003. ^{10}Be/^{7}Be tracer of atmospheric transport and stratosphere-troposphere exchange. J. Geophys. Res. 108 (D8), 4234.

Koch, D., Rind, D., 1998. Beryllium 10/beryllium 7 as a tracer of stratospheric transport. J. Geophys. Res. 103, 3907–3918.

Kovaltsov, G.A., Usoskin, I.G., 2010. A new 3D numerical model of cosmogenic nuclide ^{10}Be production in the atmosphere. Earth Planet. Sci. Lett. 291, 182–188.

Lal, D., 1987. ^{10}Be in polar ice: data reflect changes in cosmic ray flux or polar meteorology. Geophys. Res. Lett. 14, 785–788.

Lal, D., Peters, B., 1967. Cosmic ray produced radioactivity on the Earth. In: Flugge, S. (Ed.), Handbuch der Physik, vol. 46. Springer, pp. 551–612.

Lockwood, M., Bell, C., Woollings, T., Harrison, R.G., Gray, L.J., Haigh, J.D., 2010. Top-down solar modulation of climate: evidence for centennial-scale change. Environ. Res. Lett. 5, 034008.

Masarik, J., Beer, J., 2009. An updated simulation of particle fluxes and cosmogenic nuclide production in the Earth's atmosphere. J. Geophys. Res. 114, D11103.

Mavromichalaki, H., Paouris, E., Karalidi, T., 2007. Cosmic-ray modulation: an empirical relation with solar and heliospheric parameters. Sol. Phys. 245, 369–390.

Mazaud, A., Laj, C., Bender, M., 1994. A geomagnetic chronology for Antarctic ice accumulation. Geophys. Res. Lett. 21, 337–340.

Moraal, H., Muscheler, R., du Plessis, L., Kubik, P.W., Beer, J., McCracken, K.G., McDonald, F.B., 2005. ^{10}Be concentration in the Ice Shelf of Queen Maude Land, Antarctica. S. Afr. J. Sci. 101, 299–301.

Morgan, V.I., Wookey, C.W., Li, J., van Ommen, T.D., Skinner, W., Fitzpatrick, M.F., 1997. Site information and initial results from deep ice drilling on Law Dome, Antarctica. J. Glaciol. 43, 3–10.

Mosley-Thompson, E., Readinger, C.R., Craigmile, P., Thompson, L.G., Calder, C.A., 2005. Regional sensitivity of Greenland precipitation to NAO variability. Geophys. Res. Lett. 322, L24707.

Mudelsee, M., 2003. Estimating Pearson's correlation coefficient with bootstrap confidence interval from serially dependent time series. Math. Geol. 35 (6), 651–665.

Muscheler, R., Heikkilä, U., 2011. Constraints on long-term changes in solar activity from the range of variability of cosmogenic radionuclide records. Astrophys. Space Sci. Trans. 7, 355–364.

Muscheler, R., Joos, F., Beer, J., Müller, S.A., Vonmoos, M., Snowball, I., 2007a. Reply to the comment by Bard et al. on "Solar activity during the last 1000 yr inferred from radionuclide records". Quat. Sci. Rev. 26, 2304–2308.

Muscheler, R., Joos, F., Beer, J., Müller, S.A., Vonmoos, M., Snowball, I., 2007b. Solar activity during the last 1000 yr inferred from radionuclide records. Quat. Sci. Rev. 26, 82–97.

Nishiizumi, K., Imamura, M., Caffee, M.W., Southon, J.R., Finkel, R.C., McAninch, J., 2007. Absolute calibration of ^{10}Be AMS standards. Nuclear Instruments and Methods in Physics Research Section B 258, 403–413.

O'Brien, K., de La Zerda Lerner, A., Shea, M.A., Smart, D.F., 1991. The production of cosmogenic isotopes in the Earth's atmosphere and their inventories. In: Sonett, C.P., Giampapa, M.S., Matthews, M.S. (Eds.), The Sun in Time, pp. 317–342.

Palmer, A.S., van Ommen, T.D., Curran, M.A.J., Morgan, V., Souney, J.M., Mayewski, P.A., 2001. High-precision dating of volcanic events (A.D. 1301–1995) using ice cores from Law Dome, Antarctica. J. Geophys. Res. 106, 28089–28096.

Pedro, J., van Ommen, T., Curran, M., Morgan, V., Smith, A., McMorrow, A., 2006. Evidence for climate modulation of the ^{10}Be solar activity proxy. J. Geophys. Res. 111, D21105.

Pedro, J.B., Heikkilä, U.E., Klekociuk, A., Smith, A.M., van Ommen, T.D., Curran, M.A.J., 2011b. Beryllium-10 transport to Antarctica: results from seasonally-resolved observations and modeling. J. Geophys. Res. 116, D23120.

Pedro, J.B., Smith, A.M., Simon, K.J., van-Ommen, T.D., Curran, M.A.J., 2011a. High-resolution records of the beryllium-10 solar activity proxy in ice from Law Dome, East Antarctica: measurement, reproducibility and principal trends. Clim. Past 7, 707–721.

Raisbeck, G.M., Yiou, F., Bourles, D., Lorius, C., Jouzel, J., 1987. Evidence for two intervals of enhanced Be-10 deposition in Antarctic ice during the last glacial period. Nature 326, 273–277.

Raisbeck, G.M., Yiou, F., Cattani, O., Jouzel, J., 2006. ^{10}Be evidence for the Matuyama–Brunhes geomagnetic reversal in the EPICA Dome C ice core. Nature 444, 82–84.

Raisbeck, G.M., Yiou, F., Fruneau, M., Loiseaux, J.M., Lieuvin, M., Ravel, J.C., 1981. Cosmogenic Be-10/Be-7 as a probe of atmospheric transport processes. Geophys. Res. Lett. 8, 1015–1018.

Raphael, M.N., 2004. A zonal wave 3 index for the Southern Hemisphere. Geophys. Res. Lett. 312, L23212.

Raphael, M.N., 2007. The influence of atmospheric zonal wave three on Antarctic sea ice variability. J. Geophys. Res. 112, D12112.

Scaife, A.A., Knight, J.R., Vallis, G.K., Folland, C.K., 2005. A stratospheric influence on the winter NAO and North Atlantic surface climate. Geophys. Res. Lett. 321, L18715.

Shapiro, A.I., Schmutz, W., Rozanov, E., Schoell, M., Haberreiter, M., Shapiro, A.V., Nyeki, S., 2011. A new approach to the long-term reconstruction of the solar irradiance leads to large historical solar forcing. Astron. Astrophys. 529, A67.

Simon, K.J., Pedro, J.B., Smith, A.M., Child, D.P., Fink, D. Reprocessing of ^{10}B-contaminated ^{10}Be AMS targets. Nuclear Instruments and Methods in Physics research Section B, http://dx.doi.org/10.1016/j.nimb.2012.07.013, in press.

Sjolte, J., Hoffmann, G., Johnsen, J., Vinther, B.M., Masson-Delmotte, V., Sturm, C., 2011. Modeling the water isotopes in Greenland precipitation 1959–2001 with the meso-scale model REMO-iso. J. Geophys. Res. 116, D18105.

Slonosky, V., Jones, P., Davies, T., 2001. Instrumental pressure observations and atmospheric circulation from the 17th and 18th centuries: London and Paris. Int. J. Climatol. 21 (3), 285–298.

Smith, A.M., Fink, D., Child, D., Levchenko, V.A., Morgan, V.I., Curran, M., Etheridge, D.M., Elliott, G., 2000. ^{7}Be and ^{10}Be concentrations in recent firn and ice at Law Dome, Antarctica. Nuclear Instruments and Methods in Physics Research Section B 172, 847–855.

Sodemann, H., Schwierz, C., Wernli, H., 2008. Interannual variability of Greenland winter precipitation sources: Lagrangian moisture diagnostic and North Atlantic Oscillation influence. J. Geophys. Res. 113, D03107.

Steig, E.J., Polissar, P.J., Stuiver, M., Grootes, P.M., Finkel, R.C., 1996. Large amplitude solar modulation cycles of ^{10}Be in Antarctica: implications for atmospheric mixing processes and interpretation of the ice core record. Geophys. Res. Lett. 23, 523–526.

Steinhilber, F., Abreu, J.A., Beer, J., Brunner, I., Christl, M., Fischer, H., Heikkila, U., Kubik, P.W., Mann, M., McCracken, K.G., Miller, H., Miyahara, H., Oerter, H., Wilhelms, F., 2012. 9400 years of cosmic radiation and solar activity from ice cores and tree rings. Proc. Natl. Acad. Sci. U.S.A. 109 (16), 5967–5971.

Steinhilber, F., Beer, J., Fröhlich, C., 2009. Total solar irradiance during the Holocene. Geophys. Res. Lett. 36, L19704.

Trouet, V., Esper, J., Graham, N.E., Baker, A., Scourse, J.D., Frank, D.C., 2009. Persistent positive north atlantic oscillation mode dominated the medieval climate anomaly. Science 324 (5923), 78–80.

Turner, J., 2004. The El Niño-Southern Oscillation and Antarctica. Int. J. Climatol. 24, 1–31.

Usoskin, I.G., Alanko-Huotari, K., Kovaltsov, G.A., Mursula, K., 2005. Heliospheric modulation of cosmic rays: monthly reconstruction for 1951–2004. J. Geophys. Res. 110, A12108.

Usoskin, I.G., Bazilevskaya, G.A., Kovaltsov, G.A., 2011. Solar modulation parameter for cosmic rays since 1936 reconstructed from ground-based neutron monitors and ionization chambers. J. Geophys. Res. 116, A02104.

Usoskin, I.G., Horiuchi, K., Solanki, S., Kovaltsov, G.A., Bard, E., 2009. On the common solar signal in different cosmogenic isotope data sets. J. Geophys. Res. 114, A03112.

Usoskin, I.G., Mursula, K., Solanki, S.K., Schüssler, M., Kovaltsov, G.A., 2002. A physical reconstruction of cosmic ray intensity since 1610. J. Geophys. Res. 107 (A11), 1374.

van Ommen, T.D., Morgan, V., 2010. Snowfall increase in coastal east antarctica linked with southwest Western Australian drought. Nat. Geosci. 3, 267–272.

Vieira, L.E.A., Solanki, S.K., Krivova, N.A., Usoskin, I., 2011. Evolution of the solar irradiance during the Holocene. Astron. Astrophys. 531, A6.

Vinther, B.M., Johnsen, S.J., Andersen, K.K., Clausen, H.B., Hansen, A.W., 2003. NAO signal recorded in the stable isotopes of Greenland ice cores. Geophys. Res. Lett. 30 (7), 1387.

Vonmoos, M., Beer, J., Muscheler, R., 2006. Large variations in Holocene solar activity: constraints from ^{10}Be in the Greenland Ice Core Project ice core. J. Geophys. Res. 111, A10105.

Wagner, G., Laj, C., Beer, J., Kissel, C., Muscheler, R., Masarik, J., Synal, H.-A., 2001. Reconstruction of the paleoaccumulation rate of central Greenland during the last 75 kyr using the cosmogenic radionuclides ^{36}Cl and ^{10}Be and geomagnetic field intensity data. Earth Planet. Sci. Lett. 193, 515–521.

Wagner, G., Masarik, J., Beer, J., Baumgartner, S., Imboden, D., Kubik, P.W., Synal, H.-A., Suter, M., 2000. Reconstruction of the geomagnetic field between 20 and 60 kyr BP from cosmogenic radionuclides in the GRIP ice core. Nuclear Instruments and Methods in Physics Research Section B 172, 597–604.

Webber, W.R., Higbie, P.R., 2010. What Voyager cosmic ray data in the outer heliosphere tells us about ^{10}Be production in the Earth's polar atmosphere in the recent past. J. Geophys. Res. 115, A05102.

Webber, W.R., Lockwood, J.A., 1988. Characteristics of the 22-year modulation of cosmic rays as seen by neutron monitors. J. Geophys. Res. 93, 8735–8740.

Yiou, F., Raisbeck, G.M., Baumgartner, S., Beer, J., Hammer, C., Johnsen, S., Jouzel, J., Kubik, P.W., Lestringuez, J., Stiévenard, M., Suter, M., Yiou, P., 1997. Beryllium 10 in the Greenland Ice Core Project ice core at Summit, Greenland. J. Geophys. Res. 102, 26783–26794.